On the relationship between Stokes parameters *Q* and *U* of atmospheric ultraviolet/visible/near-infrared radiation

N. A. J. Schutgens,[1] L. G. Tilstra, and P. Stammes
Royal Netherlands Meteorological Institute, De Bilt, The Netherlands

F.-M. Bréon
Commissariat à l'Energie Atomique/Directions des Sciences de la Matière/Laboratoire des Sciences du Climat et de l'Environnement, Gif sur Yvette, France

Received 18 August 2003; revised 9 February 2004; accepted 23 March 2004; published 15 May 2004.

[1] On the basis of both spaceborne measurements (Polarization and Directionality of the Earth's Reflectances (POLDER)) and radiative transfer modeling, it is shown that the polarization of reflected solar light (300–900 nm) at the top of the atmosphere is most often perpendicular and less often parallel to the plane of single scattering. In terms of the elements of the Stokes vector, $|U|$ is typically much smaller than $|Q|$ when using the single-scattering plane as reference. When using any other plane, $U(\lambda) \approx Q(\lambda) \tan 2\chi_{ss}$, with χ_{ss} being the angle of the plane of polarization with the reference plane in the case of single Rayleigh scattering. Exceptions to these findings are noted, and an error analysis of $U(\lambda) \approx Q(\lambda) \tan 2\chi_{ss}$ is presented. A simplified polarization calibration algorithm for spaceborne spectrometers like the Spectrometer for Atmospheric Cartography (SCIAMACHY) is presented using the *U*-*Q* relation studied in this paper. It is shown to be just as accurate but less sensitive to measurement error than the current operational algorithm. *INDEX TERMS:* 0360 Atmospheric Composition and Structure: Transmission and scattering of radiation; 0394 Atmospheric Composition and Structure: Instruments and techniques; *KEYWORDS:* polarization, POLDER, SCIAMACHY

Citation: Schutgens, N. A. J., L. G. Tilstra, P. Stammes, and F.-M. Bréon (2004), On the relationship between Stokes parameters *Q* and *U* of atmospheric ultraviolet/visible/near-infrared radiation, *J. Geophys. Res.*, *109*, D09205, doi:10.1029/2003JD004081.

1. Introduction

[2] Several operational satellite instruments are capable of measuring two or three elements of the Stokes vector $\{I, Q, U, V\}$ [*van de Hulst*, 1981] at the top of the atmosphere (TOA). The Global Ozone Monitoring Experiment (GOME) [*Burrows et al.*, 1999] and the Spectrometer for Atmospheric Cartography (SCIAMACHY) [*Bovensmann et al.*, 1999] need such measurements for a correct radiance calibration, while Polarization and Directionality of the Earth's Reflectances (POLDER) [*Deschamps et al.*, 1994] uses polarization data for cloud [*Bréon and Goloub*, 1998] and aerosol [*Deuzé et al.*, 2001] microphysics retrieval.

[3] The Stokes vector's first three elements are the most important. Circular polarization *V* is either zero (for Rayleigh scattering) or very small (for clouds and aerosols), compared to linear polarization [*Coulson*, 1988]. In this paper we will concentrate on the linear polarization parameters *Q* and *U*. These Stokes parameters may be expressed in *P* (degree of linear polarization; $0 \leq P \leq 1$) and χ (angle between the plane of polarization and the plane of reference; $0° \leq \chi \leq 180°$):

$$Q(\lambda) = I(\lambda)\, P(\lambda) \cos 2\chi(\lambda) \tag{1}$$

$$U(\lambda) = I(\lambda)\, P(\lambda) \sin 2\chi(\lambda), \tag{2}$$

where λ is the wavelength. As a result,

$$U(\lambda) = Q(\lambda) \tan 2\chi(\lambda). \tag{3}$$

On the basis of a limited set of radiative transfer calculations, *Aben et al.* [1996, 2003] and *Stammes et al.* [1997] have assumed that $\chi(\lambda) = \chi_{ss}$, its Rayleigh single-scattering value, in order to validate GOME polarization measurements. This of course suggests that

$$U(\lambda) = Q(\lambda) \tan 2\chi_{ss}, \tag{4}$$

where χ_{ss} is given by a simple geometrical formula [*Tilstra et al.*, 2003].

[1] Currently at Communications Research Laboratory, Tokyo, Japan.

0148-0227/04/2003JD004081$09.00

[4] If we denote the Stokes vector with respect to the single-scattering plane with a superscript ^{ssp}, its transformation to another reference plane is expressed as

$$Q(\lambda) = Q^{ssp}(\lambda)\cos 2\alpha - U^{ssp}(\lambda)\sin 2\alpha \quad (5)$$

$$U(\lambda) = Q^{ssp}(\lambda)\sin 2\alpha + U^{ssp}(\lambda)\cos 2\alpha. \quad (6)$$

Here α is the angle through which the reference plane is rotated to change from the single-scattering plane to the new plane and $\alpha = \chi_{ss} - 90°$ because $\chi_{ss}^{ssp} = 90°$. It then follows that

$$U(\lambda) = Q(\lambda)\tan 2\chi_{ss} - \frac{U^{ssp}(\lambda)}{\cos 2\chi_{ss}}. \quad (7)$$

Since χ_{ss} is determined entirely from the choice of reference plane and scattering geometry, the error introduced in U when using equation (4) is determined by the statistics of $U^{ssp}(\lambda)$. The purpose of this paper is to derive statistics of U^{ssp} (and Q^{ssp}) from POLDER data and to show a practical application of equation (4).

[5] Let us consider polarization due to a single scattering and choose the scattering plane as reference. If the incident light (of which the radiance is taken as unity) is unpolarized, the polarization of the scattered light is determined by the F_{12} component of the scattering matrix [*Mishchenko et al.*, 2002]: $Q^{ssp} = F_{12}$ and $U^{ssp} = 0$. Likewise, specular surface reflection [*Jackson*, 1975] does not contribute to U^{ssp}.

[6] It follows that only multiple scattering can cause $U^{ssp} \neq 0$. However, polarization is typically dominated by the first order of scattering. Photons that have been scattered several times will have widely different polarizations and will cancel each other's contributions to the integrated polarization. This is true for both atmospheric multiple scattering [*Chandrasekhar*, 1960] and multiple scattering in the surface layer (diffuse reflection) [*Wolff*, 1975]. The exception is formed by near-backscatter geometries where second and third orders of scattering may actually dominate polarization. Note that in such cases the degree of polarization is usually low. Thus we surmise that, quite in general, $|U^{ssp}|$ is much smaller than typical values of $|Q^{ssp}|$. This would validate equation (4).

[7] When $U^{ssp} = 0$, the sign of Q^{ssp} will determine χ^{ssp}. For $Q^{ssp} < 0$, $\chi^{ssp} = 90°$, while for $Q^{ssp} > 0$, $\chi^{ssp} = 0°$. Equations (2) and (7) show that whether $\chi^{ssp} = 90°$ or $\chi^{ssp} = 0°$, equation (4) is exact.

[8] Finally, we wish to point out that often $Q^{ssp} < 0$. The scattering matrix element F_{12} for various scatterers is shown in Figure 1. For single scattering, only scattering by cloud or aerosol particles at selected geometries can create $Q^{ssp} > 0$. Likewise, surface specular scattering will always polarize the reflected light perpendicular to the plane of scattering, $\chi^{ssp} = 90°$. The effects of atmospheric and surface multiple scattering on Q^{ssp} will be rather inconsequential for reasons already discussed. The exception, of course, will be near-backscatter geometries where single-scattering polarization tends to become very small and second and third orders of scattering dominate.

[9] The consequences of the previous considerations are twofold. First, they allow a simple algorithm for the polarization correction of, e.g., SCIAMACHY and GOME-2 [*Callies et al.*, 2000], as we will show. Second, U^{ssp} is not nearly as well suited to retrieve atmospheric or surface properties as is Q^{ssp}.

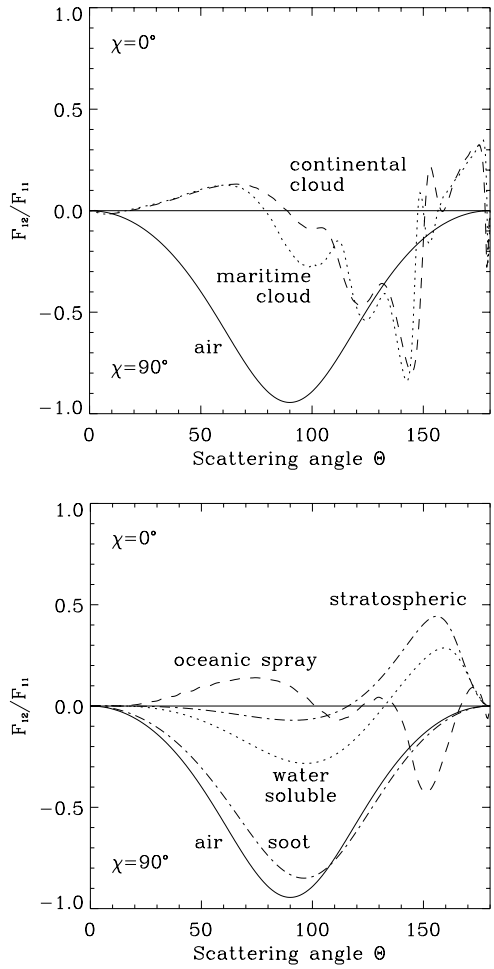

Figure 1. Scattering matrix element F_{12} (normalized to F_{11}) at 550 nm shown for different (top) cloud and (bottom) aerosol particles. Aerosol properties are taken from *Deepak and Gerber* [1983], and cloud drop properties are taken from *Miles et al.* [2000].

[10] Section 2 discusses in more detail the reference frame for the definition of the Stokes vector. Section 3 shows POLDER measurements of U and Q, while in section 4 we use radiative transfer calculations to better understand the POLDER measurements. In section 5 we discuss the relevance of this paper to the polarization calibration algorithm for SCIAMACHY. Section 6 contains the summary.

[11] The elements of the Stokes vector as used in this paper are normalized to the solar irradiance, unless noted otherwise. That is, we present the reader with $\pi Q/\mu_0 F$ and $\pi U/\mu_0 F$ where F is the solar irradiance (TOA) and μ_0 the cosine of the solar zenith angle.

2. Frame of Reference for the Stokes Vector

[12] We now turn to the definition of the reference frame for specifying a Stokes vector. The radiance I is directly

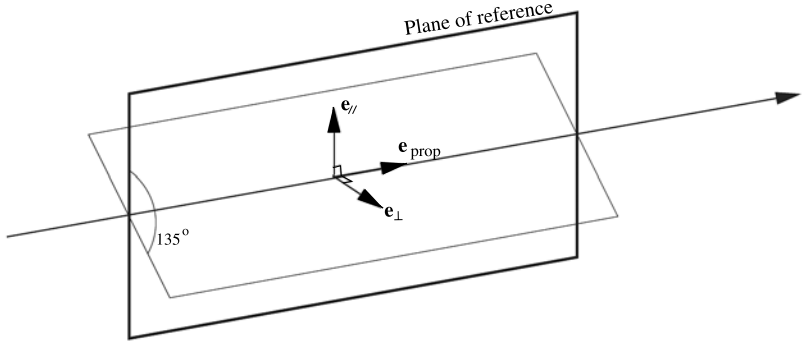

Figure 2. Definition of a reference frame for the Stokes vector. Shown are the light beam, a plane of reference, and a coordinate frame. This coordinate frame consists of $\hat{e}_{\text{prop}}$ (direction of light propagation), $\hat{e}_{\parallel}$ (lying in the plane of reference), and $\hat{e}_{\perp}$ (perpendicular to plane of reference). We have assumed $\hat{e}_{\parallel} \times \hat{e}_{\perp} = \hat{e}_{\text{prop}}$. Also shown is a (possible) plane of polarization, in this case with $\chi = 135°$. If we had assumed $\hat{e}_{\perp} \times \hat{e}_{\parallel} = \hat{e}_{\text{prop}}$, χ would have been $\chi = 45°$.

related to the magnitude of the electric field vector and thus requires no frame of reference for its definition. The other Stokes parameters,

$$Q = I_{\parallel} - I_{\perp} \tag{8}$$

$$U = I_{45°} - I_{135°}, \tag{9}$$

do require a reference plane and (in the case of *U*) a sense of rotation. The sense of rotation is usually defined by demanding that the three unit vectors $\hat{e}_{\perp}$, $\hat{e}_{\parallel}$ and $\hat{e}_{\text{prop}}$ form a right-hand coordinate frame, see Figure 2. *Chandrasekhar* [1960], *van de Hulst* [1981], and *Hovenier and de Haan* [1985] assumed $\hat{e}_{\perp} \times \hat{e}_{\parallel} = \hat{e}_{\text{prop}}$, while *Azzam and Bashara* [1987] and *Slijkhuis* [2000] assumed $\hat{e}_{\parallel} \times \hat{e}_{\perp} = \hat{e}_{\text{prop}}$. The difference in Stokes vector is the sign of *U* (and hence $\chi \rightarrow 180° - \chi$). Note that POLDER data [*Bréon and CNES Project Team*, 1997] uses the latter convention, while SCIAMACHY data [*Slijkhuis*, 1998] currently uses the first.

[13] For completeness, we also mention the definition of the scattering geometry. Four angles θ_0, ϕ_0 (solar zenith and azimuth angles) and θ, ϕ (viewing zenith and azimuth angles) are defined as shown in Figure 3. This agrees with the definition used by both our radiative transfer code and the GOME and SCIAMACHY scientific communities. The POLDER product uses a different definition of the azimuth angles. The transformation is given by

$$\text{SCIAMACHY} \quad \phi - \phi_0 \leftrightarrow 180° + \phi_0 - \phi \quad \text{POLDER}. \tag{10}$$

3. Observation of Polarization by POLDER

[14] POLDER is the only satellite instrument so far which has been capable of measuring the three top-of-atmosphere Stokes parameters {*I*, *Q*, *U*} independently at several wavelengths. POLDER was launched in 1996 onboard ADEOS-I and has operated for 8 months. During that time, polarization measurements for many different scenes were made. The observing wavelengths are in the visual and near infrared: 443, 670 and 865 nm. POLDER has a rather narrow field-of-view per pixel (0.3°) which results in a spatial resolution of 6 by 7 km at nadir. POLDER allows viewing zenith angles of $0° \leq \theta \leq 70°$. For the measurements we will present, the solar zenith angle was $0° \leq \theta_0 \leq 50°$.

[15] In Figure 4 we show the polarized Stokes parameters with respect to the single-scattering plane, Q^{ssp} and U^{ssp}. The data pertain to a large variety of scattering geometries, surfaces and atmospheric scenes during a single POLDER orbit. From Figure 4 two conclusions may be drawn at a glance: (1) $|U^{\text{ssp}}|$ is usually very small compared to typical $|Q^{\text{ssp}}|$ and (2) Q^{ssp} is usually negative.

[16] In Figure 4 we also mention the standard variation of the distribution of U^{ssp} measurements. These distributions are not shown but look very similar to Gaussian distributions. The standard deviation of U^{ssp} is typically small, on the order of 0.0015. If $U^{\text{ssp}} \neq 0$ due to multiple scattering processes (see also section 1), this value should be used with equation (7) to estimate errors in the approximation given by equation (4).

[17] However, it is very well possible that the variation in POLDER U^{ssp} is mainly due to observational errors. *Toubbé et al.* [1999] have developed a technique for calibrating POLDER's polarization measurements, using Sun glint

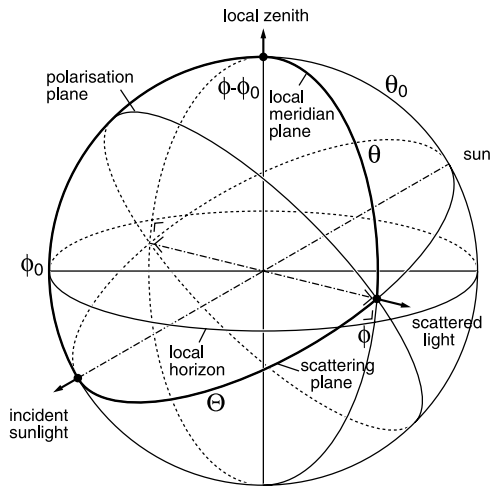

Figure 3. Definition of solar and viewing angles as used in this paper. The scattering angle is denoted by Θ.

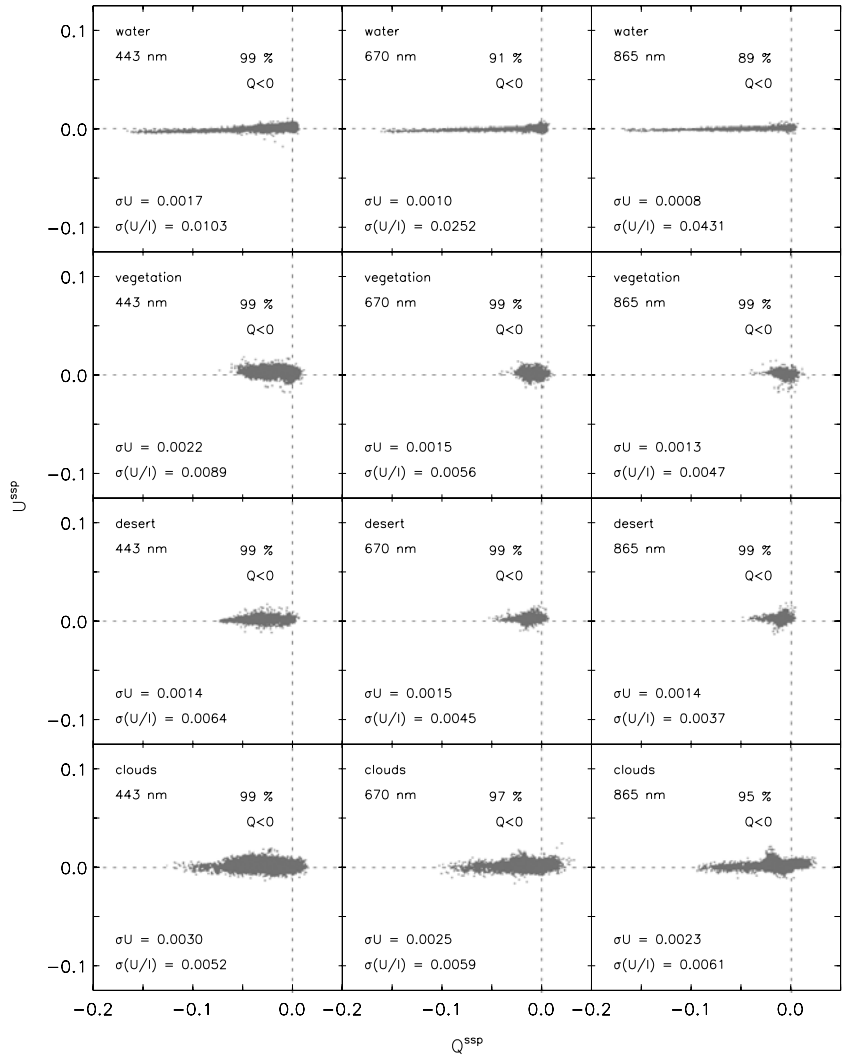

Figure 4. Polarization and Directionality of the Earth's Reflectances (POLDER) measurements of U^{ssp} and Q^{ssp} for different viewing geometries and scenes at 443, 670, and 865 nm. The standard deviations of the distributions of U^{ssp} and U^{ssp}/I are given in the lower left corner and the percentage of significantly negative Q^{ssp} in the upper right corner. Significance is here taken as the degree of polarization P being larger than three times the accuracy bounds mentioned by *Toubbé et al.* [1999]. Only cloud-free pixels were used for the water, vegetation, and desert data.

observations. They estimate they can validate POLDER's polarization measurements of Q^{ssp}/I and U^{ssp}/I with a typical accuracy of 0.005 (this error depends on both POLDER's radiometric accuracy and model assumptions). This agrees well with the standard deviations we have found (again see Figure 4) suggesting that at present, POLDER data cannot distinguish U^{ssp} from zero. The observations over water show much larger standard deviations in U^{ssp}/I than the other scenes while the variation in U^{ssp} is actually lower. This points to errors in the radiance I, which can become quite large for clear scenes over water. Note that *Toubbé et al.* [1999] used the highly reflective Sun glint for their validation algorithm.

[18] POLDER's radiometric accuracy allow errors in U^{ssp}/I and Q^{ssp}/I of 0.0015 [*Toubbé et al.*, 1999]. The true error is likely to be larger due to scene inhomogeneities. To determine U^{ssp} and Q^{ssp} three separate observations of nearly the same scene are made with differently oriented polarization filters. As POLDER moves along in its orbit, these measurements really pertain to slightly different viewing geometries and atmospheric columns. To our knowledge, no one has sofar attempted to quantify the resulting errors.

4. Modeling of Polarization

[19] For UV wavelengths $\lambda \leq 300$ nm, single scattering is actually a good approximation to radiative transfer. The strong absorption by the ozone Hartley band ensures that only single stratospheric scattering contributes to the Stokes vector at the top of the atmosphere. Barring the presence of substantial stratospheric aerosol, due to, e.g., a volcanic eruption, U^{ssp} will be zero and $Q^{ssp} < 0$. However, for most wavelengths under consideration (240–900 nm), Rayleigh single scattering is not a valid approximation.

[20] For exact nadir viewing directions, however, symmetry ensures that $U^{ssp} = 0$ irrespective of the wavelength

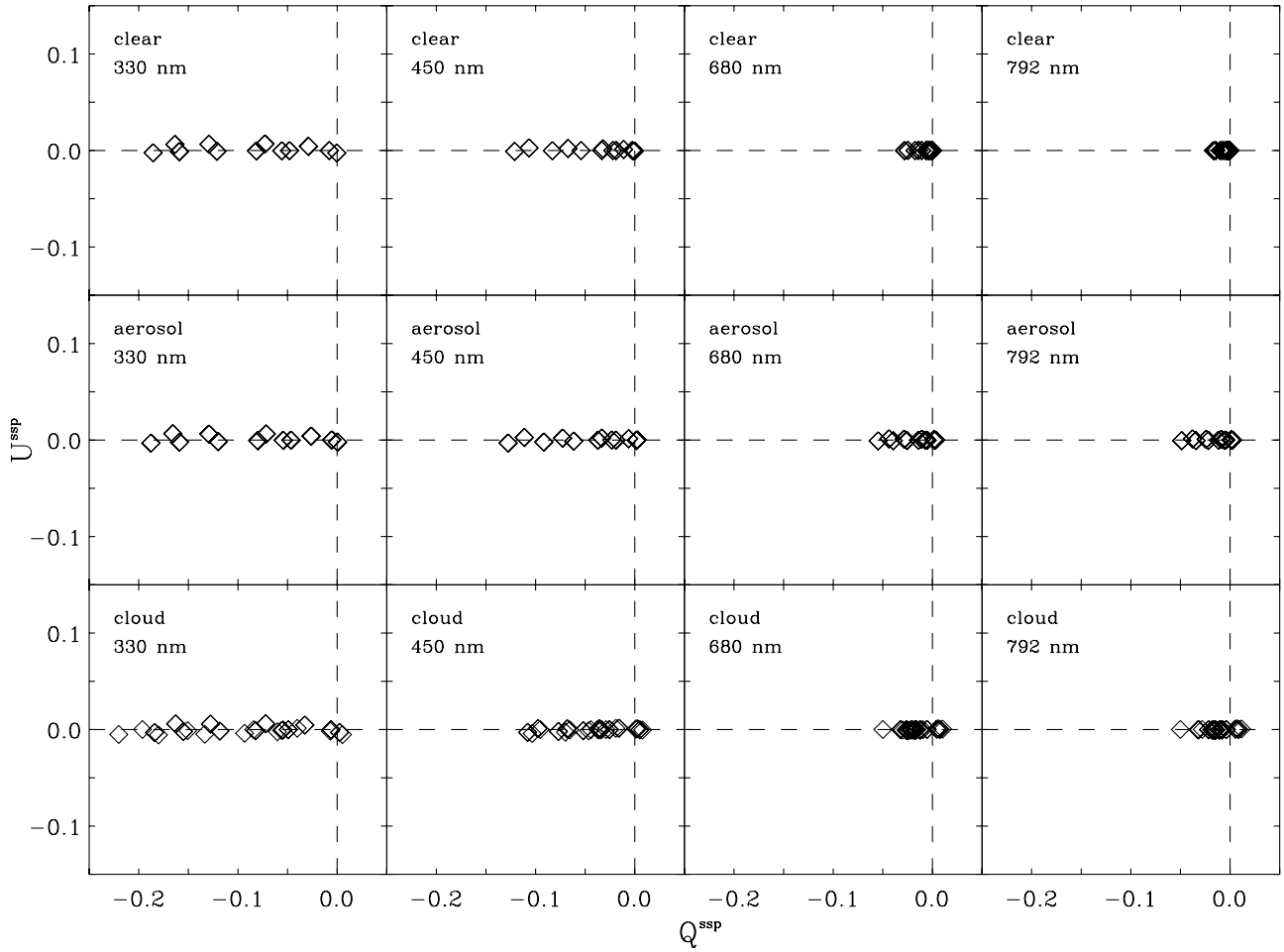

Figure 5. Radiative transfer calculations of U^{ssp} and Q^{ssp} for different scattering geometries ($\theta = 23°$ and $18° \leq \theta_0 \leq 75°$) and scenes at 330, 450, 680, and 792 nm. This figure should be compared to Figure 4. Only off-nadir viewing angles were used as observations for pure nadir result in $U^{ssp} = 0$ anyway [*Hovenier and de Haan*, 1985].

or the atmospheric scene [*Hovenier and de Haan*, 1985]. Other viewing geometries can be studied using the polarized radiative transfer model Doubling-Adding KNMI (DAK) [*de Haan et al.*, 1987; *Stammes*, 2001]. TOA Stokes vectors of reflected light (240 to 800 nm) were calculated for either clear or cloudy atmospheres or atmospheres with a substantial aerosol load. Different atmospheric profiles [*Anderson et al.*, 1986] as well as surface spectral albedos [*Bowker et al.*, 1985] were used. The surface reflection was assumed to generate unpolarized light (Lambertian surface). The calculations were made using spectrally varying (molecular) Rayleigh and (cloud and aerosol) Mie scattering properties. As DAK uses a plane-parallel atmosphere, solar zenith angles were limited to $\theta_0 \leq 75°$. The viewing angles conform to typical GOME and SCIAMACHY (nadir) viewing angles, $\theta = 0°$ or $23°$. Note that POLDER has viewing angles up to $70°$. All in all some 272 polarized spectra were calculated [*Schutgens and Stammes*, 2003].

[21] In Figure 5, we show U^{ssp} versus Q^{ssp} calculated for four wavelengths, three of which are close to the POLDER wavelengths: 450, 680 and 792 nm. Since measurement errors are not present, and numerical errors can be made arbitrarily small (at least up to machine accuracy), this figure confirms the conclusions of the previous section ($|U^{ssp}|$ much smaller than typical $|Q^{ssp}|$, and mostly $Q^{ssp} < 0$). Figures 4 and 5 differ notably in the range of Q^{ssp} values for long wavelengths. This is likely caused by POLDER observations of strongly polarized scenes due to Sun glint, while our radiative transfer code employs Lambertian surfaces.

[22] Figure 6 shows the behavior of χ^{ssp} as a function of wavelength. For most spectra χ^{ssp} shows the largest deviation from $90°$ for $300 \leq \lambda \leq 400$ nm. In this wavelength range Rayleigh multiple scattering is important. For shorter wavelengths, strong ozone absorption eliminates multiple scattering contributions to Q and U. For longer wavelengths, the Rayleigh scattering atmosphere is optically thin. Note however that χ^{ssp} never strays far from $90°$. The exceptions are three spectra shown for aerosol and cloud scenes. Each of these spectra shows strong variations in χ^{ssp}. Note that they also represent cases with very low degrees of polarization.

5. SCIAMACHY: Radiometric Calibration

[23] The relation between $Q(\lambda)$ and $U(\lambda)$ may be exploited to simplify the polarization retrieval of satellite

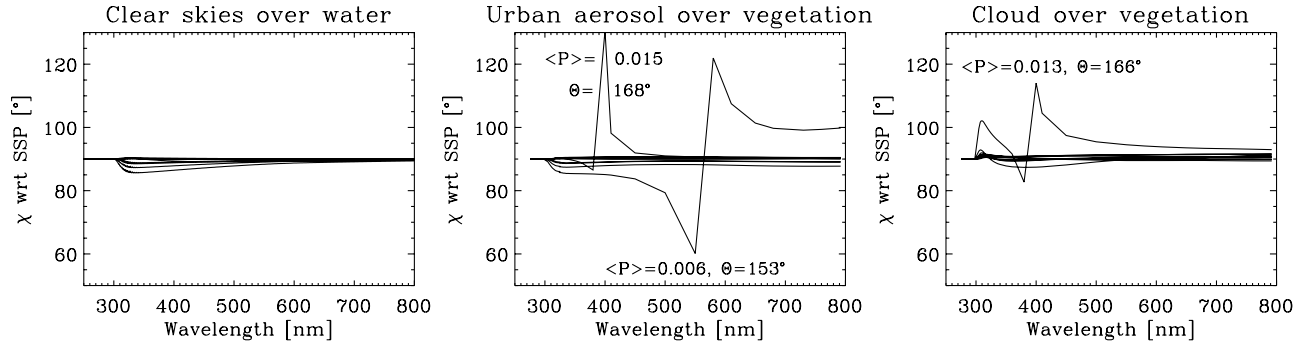

Figure 6. Calculated χ^{ssp} as a function of wavelength for three different scenes and 11 different scattering geometries ($\theta = 23°$ and $18° \leq \theta_0 \leq 75°$). The single-scattering angle is indicated by Θ. Note that χ^{ssp} only deviates strongly from 90° when the degree of polarization is low.

instruments like SCIAMACHY. This retrieval is the main step in the polarization correction of radiances [*Slijkhuis*, 1998], which in itself is one of the most important calibration issues for polarization-sensitive spectrometers [*Spurr*, 2001].

[24] The single-scattering plane is the most natural choice for reference plane. However, when discussing the results in this section the local meridian plane is more practical. This is the plane that contains the viewing and nadir directions and is used in the SCIAMACHY operational algorithms [*Slijkhuis*, 1998].

[25] SCIAMACHY yields six Q measurements (near 355, 490, 660, 850, 1580 and 2320 nm) and a single U measurement (near 850 nm). Radiance signals S are measured from 240 to 2380 nm with a high spectral resolution (0.2–1.5 nm). The calibrated radiance I is determined from

$$I = \frac{1}{M_1} \frac{S}{1 + \mu_2 Q/I + \mu_3 U/I}, \tag{11}$$

where the calibration factors M_1, μ_2 and μ_3 have been measured preflight and all parameters are wavelength-dependent. Note that this equation results from the Müller matrix expression for radiative transfer in an optical instrument [*Azzam and Bashara*, 1987]. Also note that the polarization correction becomes unimportant for unpolarized scenes. Typical values for μ_2 and μ_3 are 0.2 and −0.075, respectively (for both key data versions 2.4 and 3.0).

[26] The seven measurements of Q and U must be interpolated in wavelength as best as possible to ensure a correctly calibrated radiance. In the operational polarization retrieval, a cubic spline interpolation is used to extend the six Q measurements to the full wavelength range. Consequently, the accuracy is limited by the approximation

$$\frac{Q(\lambda)}{I(\lambda)} \approx \sum_{i=0}^{3} a_i \lambda^i. \tag{12}$$

However, interpolation of U/I can only be done using its single-scattering value at 300 nm and a measurement at 850 nm. Instead, the operational algorithm interpolates χ using its single-scattering value at 300 nm and the measurement at 850 nm. Equation (3) can then be used to determine U, from interpolated Q and χ, the idea being that χ changes less with wavelength than U/I.

[27] So, the operational algorithm uses the interpolation of χ to determine U. We, however, suggest to use the single-scattering value of χ for all wavelengths. The difference may seem small, but the simplification is useful for two reasons: (1) any χ measurement will suffer from observational errors, and at present the SCIAMACHY U measurement at 850 nm is unreliable [*Krijger and Tilstra*, 2003] and (2) it simplifies the retrieval as χ no longer needs to be determined iteratively from U and Q measurements at 850 nm but follows from a straightforward geometrical formula [*Tilstra et al.*, 2003]. For a general assessment of the error made in U when applying this simplification, see equation (7) and the discussion in section 3.

[28] Using simulated spectra (section 4), we can compare the radiance errors due to either of the two previously mentioned χ strategies. Unfortunately, our simulated data do not extend beyond 800 nm. We therefore assume only four Q measurements (near 355, 490, 660 and 800 nm) and a single (error-free) χ measurement near 800 nm. Note that the slightly reduced wavelength range can only improve the quality of the interpolation in χ. From the deviations between interpolated and true Q/I and U/I, we can derive radiance errors using SCIAMACHY's documented polarization sensitivity. Figure 7 shows a comparison of radiance errors for both χ strategies. The differences are minimal, as

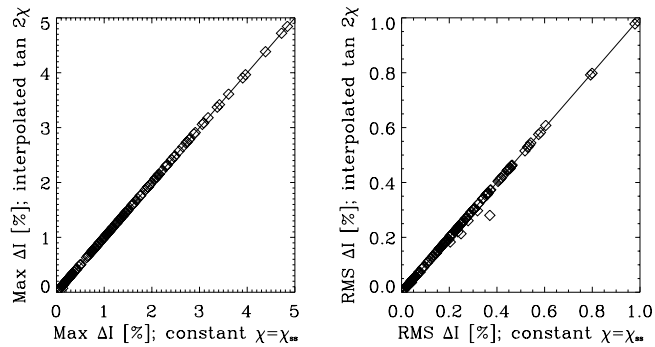

Figure 7. Comparison of radiance errors ΔI (%) (330–800 nm) in the case of the operational Spectrometer for Atmospheric Cartography (SCIAMACHY) algorithm and two different χ strategies. (left) Maximum radiance errors per spectrum. (right) RMS radiance errors per spectrum. Each diamond corresponds to a single simulated spectrum (section 4).

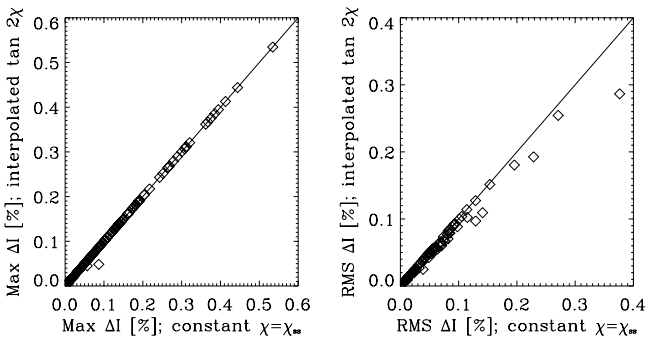

Figure 8. Comparison of radiance errors ΔI (%) (330–800 nm) in the case of the improved algorithm [*Schutgens and Stammes*, 2003] and two different χ strategies. (left) Maximum radiance errors per spectrum. (right) RMS radiance errors per spectrum. Each diamond corresponds to a single simulated spectrum (section 4).

the radiance errors are dominated by the interpolation scheme of equation (12).

[29] An improved interpolation for Q was presented by *Schutgens and Stammes* [2003]. It uses an a priori calculated Q spectrum, $Q^{\mathrm{ref}}(\lambda)$. The accuracy of the polarization retrieval is now limited by the approximation

$$\frac{Q(\lambda)}{I(\lambda)} \approx \frac{Q^{\mathrm{ref}}(\lambda)}{I(\lambda)} \sum_{i=0}^{N-1} a_i \lambda^i, \tag{13}$$

where N is the number of Q measurements. In the new algorithm, $I(\lambda)$ is determined iteratively. It was shown that, irrespective of the atmospheric scenario for which Q^{ref} was calculated, such an interpolation is superior to equation (12). Using equation (3) and either of the two χ strategies outlined above, we can implement this interpolation algorithm for SCIAMACHY as well.

[30] Figure 8 shows a comparison of radiance errors when using the improved interpolation scheme for Q. Note first the substantially smaller errors compared to Figure 7, due to the improved Q interpolation scheme. Second, there is no difference in maximum radiance errors regardless of our choice of χ strategy. A slight improvement when χ is interpolated between its theoretical value at 300 nm and a measurement at 800 nm becomes noticeable for RMS errors. It would appear that interpolation of χ leads to better radiances but only if other (e.g., Q interpolation) errors have been reduced to levels that are unattainable with the current operational algorithm.

[31] Finally, we wish to point out that both algorithms have problems dealing with situations where $\chi \approx 45°$ or 135°. In these cases $Q \approx 0$ and $\tan 2\chi$ becomes very large. An entirely different approach must then be used.

6. Summary

[32] In this paper we argue that the top-of-atmosphere Stokes parameter $|U|$ is usually much smaller than typical values for $|Q|$, and that usually $Q < 0$, where the Stokes vector is defined with respect to the single-scattering plane. We have used POLDER data as evidence and found that usually $|U| < 0.003$ (twice the typical standard variation found from Figure 4) for a variety of scenes and scattering geometries, while less than 5% of the considered POLDER data shows $Q > 0$. We argue that due to current calibration uncertainties, POLDER U cannot be distinguished from zero.

[33] A direct consequence of $|U| < 0.003$ and most $Q < 0$ is that $\chi \approx 90°$ for most viewing geometries and scenes considered. We have confirmed that $\chi \approx 90°$ through radiative transfer modeling which allows for very accurate determination of U and Q. As a drawback to radiative transfer modeling we mention that it was done for non-polarizing surfaces. This drawback is only minor as there is strong evidence in the literature that surface scattering hardly contributes to U [*Wolff*, 1975].

[34] We explain the findings in this paper by pointing out that polarization is mainly caused by single atmospheric or surface scattering and that this generally causes $U = 0$ and $Q < 0$. U may become nonzero due to multiple scattering but will remain small as higher-order scatterings tend to cancel polarization. Q may become positive due to the scattering from some cloud and aerosol particles for specific scattering geometries. In particular, backscattering geometries where second-order scattering dominates polarization [*Chandrasekhar*, 1960] are likely candidates for $\chi \neq 90°$.

[35] As a consequence, retrieval of atmospheric or surface properties using polarization measurements will not benefit from U measurements. Most information is contained in Q.

[36] We suggest that, as an application, we may use $U = Q \tan 2\chi_{\mathrm{ss}}$ in the SCIAMACHY polarization calibration, where the Stokes vector is now defined relative to the local meridian plane. The SCIAMACHY field-of-view (~4°) is small enough to allow application of our conclusions from POLDER measurements, which may be shown by integrating the Stokes vector from a single-scattering atmosphere over a finite field-of-view (exercise is left to the reader). The operational algorithm [*Slijkhuis*, 1998] interpolates χ between its single-scattering value and a measurement at 850 nm. We show that our algorithm is just as accurate as the more elaborate operational algorithm, when the latter uses an error-free χ measurement. Note that currently this χ measurement is known to be highly inaccurate [*Krijger and Tilstra*, 2003].

[37] **Acknowledgments.** The Space Research Organisation Netherlands (SRON) is acknowledged for financial support through grants EO-027 (NS) and EO-054 (LGT).

References

Aben, I., D. M. Stam, and P. Stammes (1996), Polarisation validation method applied to GOME measurements, in *IRS '96: Current Problems in Atmospheric Radiation: Proceedings of the International Radiation Symposium Fairbanks, Alaska, August 1996*, edited by W. L. Smith and K. Stamnes, pp. 506–509, A. Deepak, Hampton, Va.

Aben, I., C. P. Tanzi, W. Hartmann, D. M. Stam, and P. Stammes (2003), Validation of space-based polarization measurements by use of a single-scattering approximation, with application to the Global Ozone Monitoring Experiment, *Appl. Opt.*, *42*, 3610–3619.

Anderson, G. P., S. A. Clough, F. X. Kneizys, J. H. Chetwynd, and E. P. Shettle (1986), AFGL atmospheric constituent profiles, *Environ. Res. Pap. 954, Rep. AFGL-TR-86-0110*, Air Force Geophys. Lab., Hanscom AFB, Mass.

Azzam, R. M. A., and N. M. Bashara (1987), *Ellipsometry and Polarized Light*, Elsevier Sci., Norwell, Mass.

Bovensmann, H., J. P. Burrows, M. Buchwitz, J. Frerick, S. Noël, V. V. Rozanov, K. V. Chance, and A. P. H. Goede (1999), SCIAMACHY:

Mission objectives and measurement modes, *J. Atmos. Sci.*, *56*, 127–150.

Bowker, D. E., R. E. Davis, D. L. Myrick, K. Stacy, and W. T. Jones (1985), Spectral reflectances of natural targets for use in remote sensing studies, *NASA Ref. Publ.*, *1139*, 192 pp.

Bréon, F. M., and CNES Project Team (1997), POLDER level-1 product data format and user manual, *Rep. PA. MA.19.1332.CEA*, Cent. Natl. de Etud. Spatiales/Commissariat à l'Energ. At., Paris.

Bréon, F.-M., and P. Goloub (1998), Cloud droplet effective radius from spaceborne polarization measurements, *Geophys. Res. Lett.*, *25*, 1879–1882.

Burrows, J. P., et al. (1999), The global ozone monitoring experiment (GOME): Mission concept and first scientific results, *J. Atmos. Sci.*, *56*, 151–175.

Callies, J., E. Corpaciolli, M. Eisinger, A. Hahne, and A. Lefebre (2000), GOME-2 Metop's second generation sensor for operational ozone-monitoring, *ESA Bull.*, *102*, 28–36.

Chandrasekhar, S. (1960), *Radiative Transfer*, Dover, Mineola, N. Y.

Coulson, K. L. (1988), *Polarization and Intensity of Light in the Atmosphere*, A. Deepak, Hampton, Va.

Deepak, A., and H. E. Gerber (Eds.) (1983), World climate research programme: Report of the experts meeting on aerosols and their climatic effects, *Rep. wcp-55*, World Meteorol. Organ., Geneva, Switzerland.

de Haan, J. F., P. B. Bosma, and J. W. Hovenier (1987), The adding method for multiple scattering calculations of polarized light, *Astron. Astrophys.*, *183*, 371–391.

Deschamps, P.-Y., F.-M. Bréon, M. Leroy, A. Podaire, A. Brickaud, J.-C. Buriez, and G. Sèze (1994), The POLDER mission: Instrument characteristics and scientific objectives, *IEEE Trans. Geosci. Remote Sens.*, *32*, 598–615.

Deuzé, J. L., et al. (2001), Remote sensing of aerosols over land surfaces from POLDER-ADEOS-1 polarized measurements, *J. Geophys. Res.*, *106*, 4913–4926.

Hovenier, J. W., and J. F. de Haan (1985), Polarized light in planetary atmospheres for perpendicular directions, *Astron. Astrophys.*, *146*, 185–191.

Jackson, J. D. (1975), *Classical Electrodynamics*, John Wiley, Hoboken, N. J.

Krijger, J. M., and L. G. Tilstra (2003), Current status of SCIAMACHY polarisation measurements, *Spec. Publ. SP-531*, Eur. Space Agency, Noordjiwk, Netherlands.

Miles, N. L., J. Verlinde, and E. E. Clothiaux (2000), Cloud droplet distributions in low-level stratiform clouds, *J. Atmos. Sci.*, *57*, 295–311.

Mishchenko, M. I., L. D. Travis, and A. A. Lacis (2002), *Scattering, Absorption, and Emission of Light by Small Particles*, Cambridge Univ. Press, New York.

Schutgens, N. A. J., and P. Stammes (2003), A novel approach to the polarization correction of spaceborne spectrometers, *J. Geophys. Res.*, *108*(D7), 4229, doi:10.1029/2002JD002736.

Slijkhuis, S. (1998), SCIAMACHY level 0 to 1c processing algorithm theoretical basis document, *Tech. Note ENV-ATB-DLR-SCIA-0041*, Dtsch. Zent. für Luft- und Raumfahrt, Oberpfaffenhofen, Germany.

Slijkhuis, S. (2000), Calculation of polarisation from Rayleigh single scattering, *Rep. ENV-TN-DLR-SCIA-0043*, Dtsch. Zent. für Luft- und Raumfahrt, Oberpfaffenhofen, Germany.

Spurr, R. J. D. (2001), Linearized radiative transfer theory: A general discrete ordinate approach to the calculation of radiance and analytic weighting functions, with application to atmospheric remote sensing, Ph.D. thesis, Tech. Univ. Eindhoven, Netherlands.

Stammes, P. (2001), Spectral radiance modelling in the UV-visible range, in *IRS 2000: Current Problems in Atmospheric Radiation*, edited by W. L. Smith and Y. M. Timofeyev, pp. 385–388, A. Deepak, Hampton, Va.

Stammes, P., I. Aben, R. B. A. Koelemeijer, S. Slijkhuis, and D. M. Stam (1997), GOME polarisation validation study, paper presented at the 3rd ERS Symposium on Space at the Service of our Environment, Eur. Space Agency, Florence, Italy.

Tilstra, L. G., N. A. J. Schutgens, and P. Stammes (2003), Analytical calculation of Stokes parameters *Q* and *U* of atmospheric radiation, *Sci. Rep. WR 2003-01*, Koninklijk Ned. Meteorol. Inst., De Bilt, Netherlands.

Toubbé, B., T. Bailleul, J.-L. Deuzé, P. Goloub, O. Hagolle, and M. Herman (1999), In-flight calibration of the POLDER polarized channels using the Sun's glitter, *IEEE Trans. Geosci. Remote Sens.*, *37*, 513–525.

van de Hulst, H. C. (1981), *Light Scattering by Small Particles*, Dover, Mineola, N. Y.

Wolff, M. (1975), Polarization of light reflected from a rough planetary surface, *Appl. Opt.*, *14*, 1395–1405.

F.-M. Bréon, Commissariat à l'Energie Atomique/Directions des Sciences de la Matière/Laboratoire des Sciences du Climat et de l'Environnement, Avenue de la Terrasse, F-91191 Gif sur Yvette, France. (fmbreon@cea.fr)

N. A. J. Schutgens, Communications Research Laboratory, 4-2-1 Nukuikitamachi, Koganei, Tokyo 184-8795, Japan. (schutgens@crl.go.jp)

P. Stammes and L. G. Tilstra, Royal Netherlands Meteorological Institute, P.O. Box 201, De Bilt, NL-3730 AE, The Netherlands. (stammes@knmi.nl; tilstra@knmi.nl)